地球环境学报
Journal of Earth Environment

doi:10.7515/JEE201606005

中国北方三典型流域地表沉积物空间分异及指示

李小妹[1,2]，严　平[1,3]，吴　伟[1,3]，钱　瑶[1,3]

（1. 北京师范大学 地表过程与资源生态国家重点实验室 , 北京 100875；2. 陕西师范大学 旅游与环境学院，西安 710119；3. 北京师范大学 防沙治沙教育部工程研究中心，北京 100875）

摘　要：风水交互作用是干旱区（广义）最为广泛的一种地表现象与地貌过程。通过对西部的克里雅河、中部的毛布拉孔兑河和东部的西拉木伦河三个典型流域的实地考察、地形测量、取样，分析其地表沉积物样品的粒度、化学风化过程以及动力因素，发现：自西向东三流域的粒度特征表现为粒度变粗，分选性变差，峰态变宽，粒度的水成特性更加明显；三流域的矿物及元素风化指数表明了三流域处于化学风化的最初阶段，且自西向东三流域化学风化程度增强，物理风化程度减弱；其中，化学成分变异指数（ICV）与碳酸钙化学参数含量可以很好的区分三流域地表物质的风化特征异质性。究其原因，在流域尺度上，气候引起风和水两种营力对地表沉积物的差异性分选，使得三流域地表沉积物理化特征呈现地带性规律。

关键词：中国北方；三个流域；地表沉积物；风水交互作用

Differences of surface sediments in three basins of northern China and its implications

LI Xiaomei[1,2], YAN Ping[1,3], WU Wei[1,3], QIAN Yao[1,3]

(1. State Key Laboratory of Earth Surface Processes and Resource Ecology, Beijing Normal University, Beijing 100875, China; 2. Tourism and Environmental Sciences, Shaanxi Normal University, Xi'an 710119, China; 3. MOE Engineering Center of Desertification and Blown-sand Control, Beijing Normal University, Beijing 100875, China)

Abstract: ***Background, aim, and scope*** Interaction between aeolian and fluvial systems occurs widely on the surface of the Earth and plays an important role in the development of arid landforms, spanning spatial and temporal scales. The formation and evolution of deserts have close relations with the rivers, while aeolian dunes influence channel processes and fluvial geomorphology. ***Materials and methods*** Field investigation, topographic survey, sampling, laboratory analysis of grain size, mineral composition and chemical element were carried out on surface sediment samples from three river basins, including Keriya River in the west, Mu Bulag River in the middle, and Xi Xar Moron River in the east of northern China. ***Results*** The average grain size gradually coarsened from west to east for the three basins, the sorting worsened, the skewness increased, the kurtosis widened, and the hydrogenic characteristic became more obvious. In terms of mineral composition, the sediments were composed mainly of light mineral-based substances, especially quartz and feldspar, and the mineral maturity gradually decreased from west to east for the three basins. In terms of chemical elements,

收稿日期：2016-06-08；**录用日期**：2016-08-10

Received Date: 2016-06-08; **Accepted Date:** 2016-08-10

基金项目：国家重点基础研究发展计划（2013CB956001）；地表过程与资源生态国家重点实验室自由探索项目（2015-ZY-14）；国家自然科学基金项目（41171003）

Foundation Item: National Basic Research Program of China (2013CB956001); State Key Laboratory of Earth Surface Processes and Resource Ecology, Free Exploration Project (2015-ZY-14); National Natural Science Foundation of China (41171003)

通信作者：严　平，E-mail: yping@bnu.edu.cn

Corresponding Author: YAN Ping, E-mail: yping@bnu.edu.cn

Si, Al, and Ca elements were dominant, and other elements were less concentrated. Compared with data of upper continental crust (UCC), most elements were depleted, with the exception of Si, Ca, and Co, and the self-enrichment level and loss level of these elements gradually increased. In addition, the variation coefficients also gradually increased from west to east for the three basins, indicating that the post-weathering effect on the three basins gradually increased. The chemical index of alteration (CIA) in the three basins was generally less than 50, and A-CN-K diagrams indicated that the three basins were in the initial chemical weathering stage and the weak loss stage of Ca and Na. Other elements did not show obvious signs of chemical weathering or migration. A-CNK-FM diagrams showed that Fe and Mg in the three basins underwent significant differentiation, and the effects of physical and chemical weathering on sediment characteristics were different. Analysis of the grain size and chemical weathering parameters showed that the grain size sensitive components, the standard deviation, the index of chemical variability (ICV), and the $CaCO_3$ content could be used to properly distinguish the characteristic heterogeneity of the weathering of surface substances in the three basins. ***Discussion*** The controlling factors upon sediments features, which include source rock, structure, the physical and chemical weathering caused by the climate and depositional topography, vary with different spatial scales. In the large-scale basins, the climatic factors are quite important in the weathering of surface sediments, which presents as the relative coherence of the variation rules from the west to the east as well as in a certain basin. This does not only lie on the basic component of the substance in the source area, but also on the differences in the later weathering. In Keriya River, the hot and dry environment lead to the lack of surface chemical processes but it is mechanically reshaped by the wind (high sorting and blending). The surface sands in Mu Bulag River and Xi Xar Moron River have experienced chemical change to some extent, which might be related to the near-surface water and the underground water. In the middle-scale river reach, differentiations in the sorting of sand and the pattern of certain elements are caused by the pattern and flow direction of the river, the wind direction, the local topography because they can influence the strength of the aeolian-fluvial agent. In the small-scale river cross-section, the differentiations result mainly from seasonal floods, the relation between local wind regime and flow direction, rivers concavity and convexity, the distance away from the river reach etc. ***Conclusions*** The combination and conversion between different spatial scales depend on the sediments by the aeolian-fluvial interactions. The mode and degree of the aeolian-fluvial interaction are different in varying spatial scale. But the features of surface sediments are gradually transformed by the aeolian-fluvial processes, forming a similarity which is hard to distinguish. ***Recommendations and perspectives*** Therefore, it is more urgent to establish a proper index to discriminate aeolian and hydromorphic origins of sediments and their relation in sedimentology and material source in the dryland system.

Key words: northern China; three basins; surface sediments; aeolian-fluvial interactions

1 Introduction

Arid zone geomorphology is a product by long-term interactions of various agents including water and wind (Tooth, 2008). Recently, increasing works have concentrated on aeolian-fluvial interactions in dryland environments, and the associations between deserts and rivers landforms and its connectivity (Bullard and Livingstone, 2002; Field et al, 2009; Ravi et al, 2010; Belnap et al, 2011), recognized the important role of rivers in providing sand provenances and spaces for deserts development (Bullard and McTainsh, 2003; Draut, 2012), as well as the influences and controlling of aeolian activity upon river landforms (Tooth and Nanson, 2011). The interaction between wind and water varied at different spatial and temporal scales, and stratigraphic studies indicated that climate and topography were two key factors controlling this pattern (Bullard and Livingstone, 2002; Field et al, 2009; Ravi et al, 2010). The grain size distributions of dune sands have acted as an important factor on the morphology and dynamic processes of dunes (Bagnold and Barndorff-Nielsen, 1980; Lancaster, 1995). Grain size has been one of the major parameters described when the history of the development of the sand seas is considered (Thomas, 1988; Lancaster, 1989; Winspear and Pye, 1995). Furthermore, the grain size characteristics of the dune sands are closely related to factors such as dynamic processes of the dunes, sand availability, vegetation, and the transportation distances from the source zones (Lancaster, 1995). Soil results from weathering, or the combined actions of hydrosphere, biosphere and atmosphere on rock materials (Churchman, 2000). In sand seas minerals in soils may often form not from local rock, but from detrital sediments which are transported from other parent rock sources. The degree of chemical weathering of these detrital sediments is therefore indicative of the history of soil formation in sandy deserts. In addition, mineralogical and geochemical studies of dune sands provide new insights into the origin and evolution of aeolian sand bodies (Muhs, 2004). Recent works of modern surface sediment has focused mainly on sources of inland desert sand (Nesbitt and Young, 1996; Li, 2011; Xu et al, 2011), while the transition zone from deserts to rivers, in which wind and water significantly interact, has received less attention. Because of the geomorphologic responses to the recurring wind and water interactions and subsequent sedimentary processes, sediment composition in this zone became uncertain and complex and, thus, could be studied by regional comparison. Feature study on surface sediments near different rivers could be conducted for comparison of sediment behaviors in different dynamic combinations of wind and water.

In this paper, Keriya River in the west, Mu Bulag River in the middle, and Xi Xar Moron River in the east were chosen as study areas that represent typical river basins in northern China (Fig.1). The grain size composition characteristics of surface sediments, spatial distribution of mineral substances and geochemical elements, and surface weathering processes in the three basins were comprehensively compared and analyzed. Furthermore, we explored the indication of surface sediment on the aeolian-fluvial environments and its significance on the origin and development of deserts. This paper examines the physical and chemical character of aeolian sediments under arid climatic conditions, and to determine possible factors controlling the weathering process in a dynamic basins of sand sea. A deep understanding of the weathering process (chemical weathering and physical weathering) by water or wind is crucial to the interpretation of regional geomorphological evolution (Condie et al, 1995; Nesbitt and Markovics, 1997).

2 Materials and Methods

2.1 Study areas

The Keriya River (Fig.1) is located at the southern edge of the Tarim Basin, Xinjiang and originates in the northern slope of Wusitentag Mountain, the main Peak of the Kunlun Mountains. It flows northward into the Taklimakan Desert hinterland, and finally disappears near Daria Boyi. The total length of the river is 860 km (including the 90 km abandoned channel), of which 350 km flows through the desert, and the total basin area reaches 39500 km^2. The terrain of the basin decreases from south to north, along which sediments can be divided into four geomorphic units, desert, Gobi, foothill and glaciated mountain (Yang et al, 2002). The climate is warm temperate continental, with an annual average rainfall of 45 mm and an annual average temperature of 11.6℃ .

The Mu Bulag River (Fig.1) is a first-grade tributary of the Yellow River and originates in Amenchijihko of Hangchin Banner, Inner Mongolia. It has a mainstream length of 111 km, a basin area of 1300 km^2, and an annual average discharge of $7.57\times10^6\ m^3\cdot a^{-1}$. Its middle and lower sections pass across the Hobq Desert. Its terrain decreases from south to north and from west to east with an elevation of 1000 —1500 m, and the sediments can be divided from south to north as three zones, loess hill, Hobq Desert, alluvial plain of the Yellow River. It has a semi-arid steppe climate, with an average annual rainfall of 241 mm and an annual average temperature of 5.9℃ .

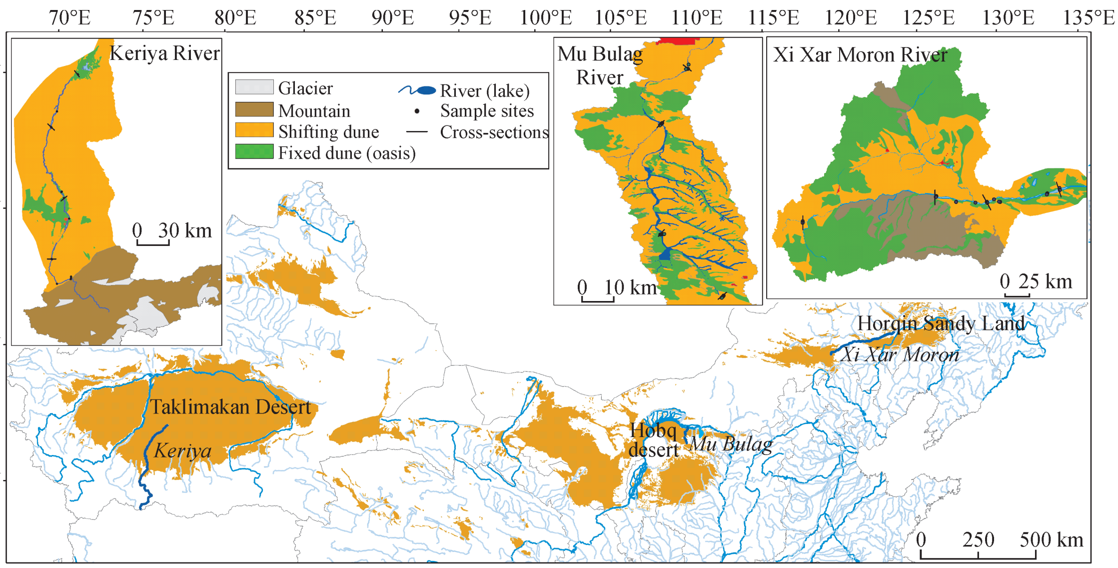

Fig.1 Sketch map of sample sites in the three river basins of northern China

The Xi Xar Moron River (Fig.1) flows into the Xiliao River and originates in Baicha Mountain in Hexigten Banner, Inner Mongolia. It has a full length of approximately 380 km and a total basin area of 32200 km^2. The river has an intermediate temperate continental monsoon climate, with an annual average rainfall of approximately 400 mm and an annual average temperature of 5—7℃ .

2.2 Sampling and topographic survey

According to data of three river basins and field investigation, we selected four typical river sections from each of Keriya, Mu Bulag, and Xi Xar Moron Rivers, i.e. upper reaches, middle reaches, lower reaches and end of river, and sampled with cross-sectional topographic survey in July and October 2013 (Fig.1). Beside those cross-sectional samples, other surface sediments were collected between them. All surface samples of 500 —1000 g each were gathered at 0—5 cm depth. Sampled sediments included riverbed alluvial, floodplain deposition, aeolian sand on terrace. A total of 364 samples were collected in the three basins, of which 93 samples from the Keriya River, 129 samples from the Mu Bulag River, and 142 samples from the Xi Xar Moron River.

2.3 Experimental analysis

Geochemical study was carried out in the Key Laboratory of Desert and Desertification, Cold and Arid Regions Environmental and Engineering Research Institute, Chinese Academy of Sciences. Samples were prepared by pressing disc method. The air-dried samples were grinded to 200 meshes, and 4-g powered sub-samples were placed into the mold with boric acid for the edge and bottom after dried at 105℃ , and pressed under 30 tons into a 32-mm diameter discs. The discs were measured with a sequential wavelength dispersive X-ray Fluorescence Spectrometer (Panalytical Axios PW4400). The main elements contents were expressed as oxide percentages and the trace element contents as μg/g, with estimated error less than 5%.

The grain size of those samples were tested by a Malvern Mastersizer 2000 particle size analyzer at the State Key Laboratory of Earth Surface Processes and Resource Ecology in Beijing Normal University. The grain size analysis was performed with a Laser Particle Size Analyser that determines the particle sizes between –1.0 φ and 14.6 φ. Particle size distributions were given in μm and converted into φ units to calculate the grain size distribution parameters with the formula Log2 (mm) and percentiles utilized in Folk’s formulae (Folk, 1980) . The size paraments were calculated by formula of Folk and Ward (1957). At the Analysis and Testing Center of Beijing Normal University, $CaCO_3$ content was measured by the gasometric method which $CaCO_3$

standard curve was created to calculate the percentage of $CaCO_3$ in each sample.

49 samples were chosen, 1—2 samples of each sediment type from the four cross-sections, were used for mineral substances. The 30-g powered sub-samples were tested by X-ray diffractometer (X'pert PRO) at the Ministry of Education Key Laboratory of Western Environment, Lanzhou University. The main mineral substances in each sample were determined from the sizes of the diffraction peaks, and the percentage composition of each substance was calculated with the semi-quantitative analysis method by Biscaye (1965).

3 Results and Analysis

3.1 Grain size composition and parameters

As shown in Tab.1 and Fig.2, both clay (<4 μm) and very coarse sand (1000—2000 μm) content were low in surface sediments of the three basins. In the Keriya River, very fine sand (63—125 μm) content was highest at 44.17%, followed by silt (4—63 μm) and fine sand (125—250 μm) over 20% each, and medium sand (250—500 μm) and coarse sand (500—1000 μm) contents were less, very coarse sand was not detected. In the Mu Bulag River, fine sand content was the highest at 41.28%, followed by medium sand and very fine sand at 25.16% and 19.72%; the silt and very coarse sand contents were less. In the Xi Xar Moron River, the fine sand and medium sand contents dominated at 29.72% and 26.45%, followed by very fine sand and silt at 20.07% and 15.63%, and the coarse sand content was less. Overall, from west to east for three basins, the silt and very coarse sand contents were decreased, while the fine sand and medium coarse sand contents were increased, and the average particle size became coarser. As for the other grain-size parameters for the three basins (Tab.1), the sorting (standard deviation) was 0.87—1.07 φ, moderately sorted to poorly sorted, the skewness was 0.07—0.17, symmetrical to fine skewed, the kurtosis was 1.11—1.23, leptokurtic. From west to east, the sorting tended to poorer, the skewness to more symmetrical, and the kurtosis to wider.

Tab.1 Grain size composition and parameters of surface sediments in the three basins

Basin	Percentage of each size/%							M_z/φ	σ_I/φ	SK_1	K_G
	Clay (<4 μm)	Silt (4—63 μm)	Very fine sand (63—125 μm)	Fine sand (125—250 μm)	Medium sand (250—500 μm)	Coarse sand (500—1000 μm)	Very coarse sand (1000—2000 μm)				
Keriya River	0.70	25.64	44.17	23.55	4.64	0.76	0.00	3.52	0.87	0.07	1.11
Mu Bulag River	0.72	8.62	19.72	41.28	25.16	4.18	0.31	2.55	1.01	0.15	1.23
Xi Xar Moron River	1.20	15.63	20.07	29.72	26.45	6.82	0.11	2.70	1.07	0.17	1.21

3.2 Mineral composition

Light mineral is dominant content in the three basins while heavy mineral account for less. The major component of light mineral was quartz and feldspar, and of the heavy mineral was biotite (Fig.3). In the Keriya River, the quartz content was highest, accounting for approximately 55%, followed by biotite, 15%. In the Mu Bulag River, the quartz content was highest, accounting for approximately 50%, followed by feldspar and biotite, which together contribute 40%. In the Xi Xar Moron River, the biotite content was highest, accounting for approximately 45%, followed by the quartz, 30%. From west to east for the three basins, the quartz content decreased, while the biotite and the feldspar increased. Quartz and feldspar had smaller variations, while calcite and dolomite had larger variations. The variation coefficient for the Keriya

River was smaller, while the variation coefficients for the Mu Bulag River and Xi Xar Moron River were larger, indicating that the mineral composition for the former was relatively simple and the two latter were more complex. The major differences in mineral composition in the three basins may be related to the mineral composition of the original rock and different weathering conditions.

The major component of heavy minerals in the three basins were unstable minerals (biotite and amphibole), and only small contribution from stable minerals (epidote), which indicate that the sediments experiencing short-term secondary alteration. The boundaries of the mineral maturity indices (the ratio of feldspar to quartz) in the three basins were obvious, and the distribution of samples was relatively concentrated in each basin (Fig.4). The order of the feldspar/quartz ratio were Keriya River < Mu Bulag River < Xi Xar Moron River, indicating that mineral maturity decreased from west to east. Thus, the surface sediments in the western basin were more mature and experienced long-term transformation than ones in the eastern basin. In addition, the more arid climate in the western basin caused sediments to update slowly, while new materials were transported and complemented frequently in the eastern basin, which was one of the most important reasons for the young age of sediments near the rivers.

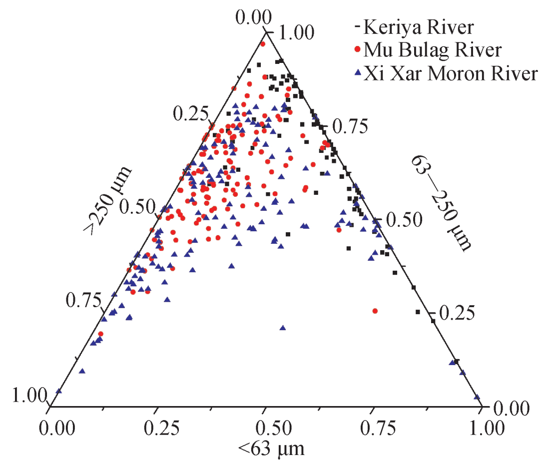

Fig.2 Ternary diagram of grainsize composition in the three basins

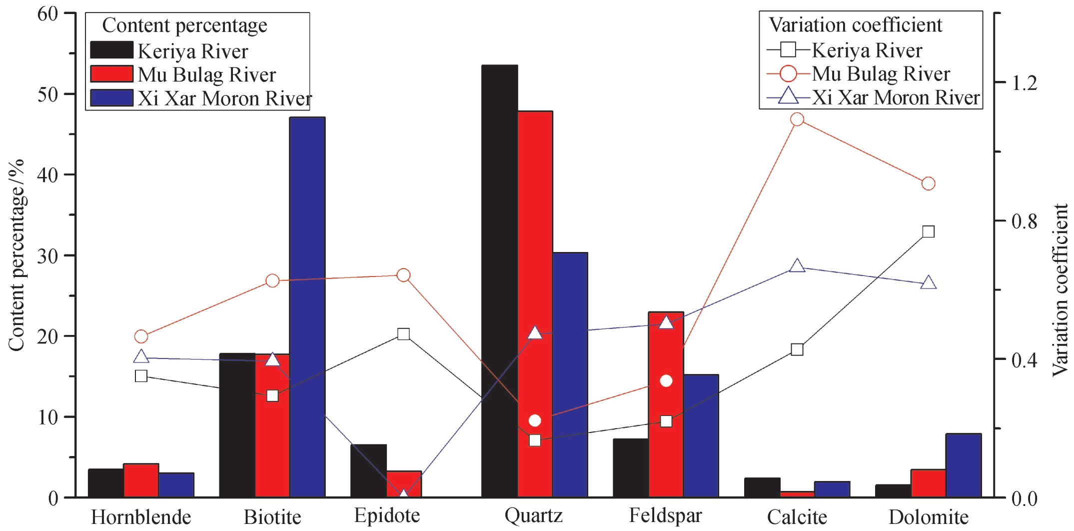

Fig.3 Mineral content histogram and variation coefficient line chart for the three basins

3.3 Chemical element component

The constant oxides of surface sediments in the three basins included SiO_2, Fe_2O_3, $A1_2O_3$, CaO, MgO, K_2O, and Na_2O (Tab.2). Of these, SiO_2 content was the highest (60.5%—86.5%), followed by $A1_2O_3$ (7.5%—9.7%), and all other oxides were less concentrated. The sediments also contained 19 different trace elements, including Ti, Ba, Sr, and Co, among which the Ti highest (0.19%—0.29%), followed by Ba (0.055%—0.068%), and all other trace elements were less concentrated. Compared with UCC (Fig.5), the SiO_2 content of sediments from the three basins was close that of the UCC, and for trace elements, Co (6.11—19.45) and As (3.37—5.51) were enriched, while Ni, Zr, Ce, Rb and Ba were similar to the UCC. From the differences observed between element distribution curves for the three basins, the change magnitude for the Keriya River was smaller than those for the Mu Bulag River and Xi Xar Moron River, which were similar to each other. The CaO and MgO contents of the Keriya River were enriched, while the CaO and MgO contents of the Mu Bulag River and Xi Xar Moron River were depleted. The enriched CaO in the Keriya River was likely related to the large amount of carbonate minerals (calcite and dolomite) contained in the original rock sediment. In addition, the arid climate made CaO less likely to be dissolved by rain and, thus, enriched at the surface. The more stable losses of Al_2O_3 and Fe_2O_3 in sediments from the three basins were related to the low bauxite and iron mineral content of the original rock sediment. A large amount of silicate debris and highly dispersed silicates (such as feldspar, mica, etc.) were enriched in the arid and semi-arid sand sediments, which diluted the trace element content, but their change magnitudes were relatively small (Dobrovoljski, 1987).

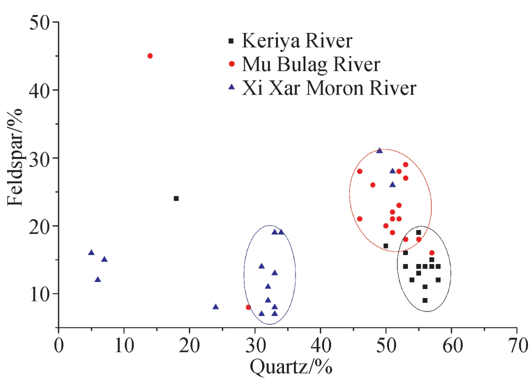

Fig.4 Mineral distribution scatter diagram for the three basins

As seen from the variation coefficient, most elements had moderate variation (CV =0.1—1.0), with the exception of SiO_2, Sr, and several other elements, which displayed weak variation (CV <0.1). In addition, the element variation degree increased from west to east for the three basins.

3.4 Weathering degree index

The SiO_2/Al_2O_3 ratio can be used to indicate the weathering extent of quartz mineral, and Na_2O/K_2O ratio can be used to indicate the relative losses of Na-feldspar to K-feldspar, which are often used as indices of the chemical weathering degree (Robinson and Johnsson, 1997). The ICV is used to reflect the degree of chemical of minerals using the following formula by Cox (1995). Compared with clay minerals, non-clay minerals have a higher ICV value, and the ICV value of the terrestrial crust is 1.5. An ICV value of >1 for sediments indicates that the sediment clay content is low and suggests that the sediment originated from the first deposition in the mobile construction zone (Cullers and Podkovyrov, 2000; Cullers, 2002). An ICV value of <1 in sediments indicates that a large amount of clay minerals are present and suggests that the sediment originated from the first deposition under recycling or intense chemical weathering conditions (Cox, 1995).

As seen from both scatter plots (Fig.6a), the weathering degree of feldspar minerals in the three basins can be sequenced as Xi Xar Moron River > Mu Bulag River > Keriya River. Contrastingly, the weathering degree of quartz minerals as Keriya River > Mu Bulag River > Xi Xar Moron River, indicating that physical weathering was weakened and chemical weathering was enhanced from west to east for the three basins. The boundaries of the SiO_2/Al_2O_3 and Na_2O/K_2O ratios between Keriya River and Mu Bulag River were 7.5 and 1.5 respectively, and roughly 10.0 and 1.0 between Mu Bulag River and Xi Xar Moron Rive despite their partly overlapping.

$CaCO_3$ content is used as a measure of climate and weathering (Lancaster, 1995; Gile et al, 1996; Li and Yang, 2004). As seen from the $CaCO_3$ and ICV scatter plot (Fig.6b), $CaCO_3$ content was 4.63—13.08%, and ICV was 0.7—3.0. ICV and $CaCO_3$ content both decreased from west to east for the three basins, indicating that the chemical weathering degree increased. The ICV was < 1 in the Xi Xar Moron River, 1—1.5 in the Mu Bulag River, and > 1.5 in the

Keriya River, which was reflective of the increase in the chemical weathering degree from west to east (Cullers and Podkovyrov, 2000). The $CaCO_3$ content gradually decreased from west to east in the three basins, indicating that the chemical weathering degree gradually increased. The boundaries of $CaCO_3$ content were approximately 6% and 9% between Xi Xar Moron Rive, Mu Bulag River and Keriya River respectively.

Tab.2 Element content (%) and variation coefficient statistics in the three basins

Elements	Keriya River			Mu Bulag River			Xi Xar Moron River			Average UCC
	Range	Average	Variation	Range	Average	Variation	Range	Average	Variation	
SiO_2	51.50—67.94	60.52	0.056	67.77—89.40	78.89	0.04	56.99—95.48	86.52	0.08	66.00
Al_2O_3	8.75—12.87	9.63	0.066	7.04—11.16	9.64	0.10	4.2—14.74	7.53	0.23	15.20
Fe_2O_3	2.57—5.56	3.21	0.171	1.03—3.53	2.04	0.25	0.31—6.35	1.18	0.67	5.00
MgO	1.78—4.08	2.43	0.179	0.28—1.91	0.65	0.39	0.12—2.45	0.34	0.94	2.20
CaO	4.95—9.73	8.12	0.132	1.02—5.68	2.82	0.34	0.24—4.88	0.91	0.72	4.20
Na_2O	2.37—6.62	3.67	0.193	1.9—3.73	2.85	0.16	1.17—3.97	2.07	0.30	3.90
K_2O	1.89—2.69	2.06	0.058	1.85—2.99	2.4	0.12	1.75—3.38	2.76	0.12	3.4
Cl	48.63—13891.20	1523.28	1.808	25.34—1821.25	94.51	2.60	19.33—616.31	42.20	1.56	640.00
P	369.25—787.31	564.08	0.180	221.78—519.16	341.62	0.20	142.49—740.87	225.90	0.39	665.00
Ti	2264.00—4328.00	2943.97	0.120	981.42—3671.43	2261.29	0.25	628.08—4676.42	1893.93	0.46	3000.00
V	46.71—92.73	57.31	0.150	16.16—69.86	39.01	0.28	3.09—105.51	26.78	0.61	60.00
Cr	37.58—98.07	48.65	0.210	15.47—65.29	34.71	0.28	8.68—77.66	23.26	0.45	35.00
Mn	390.61—777.09	503.89	0.130	143.01—524.64	301.31	0.23	65.55—1015.73	208.01	0.58	600.00
Co	31.58—107.78	61.11	0.190	92—207.49	141.29	0.15	39.67—367.11	194.07	0.32	10.00
Ni	21.06—45.47	27.46	0.160	19.7—30.76	23.97	0.09	18.41—46.02	25.10	0.14	20.00
Cu	12.69—41.22	17.27	0.220	5.22—18.16	9.35	0.22	3.32—37.70	7.06	0.60	25.00
Zn	15.69—83.09	29.34	0.340	/	0.44	14.78	/	2.06	13.97	71.00
Ga	10.77—16.85	12.15	0.080	8.28—14.52	11.91	0.10	6.84—20.27	9.73	0.20	17.00
As	5.05—25.2	8.27	0.390	4.28—10.72	0.19	0.19	3.3—22.03	5.65	0.34	1.50
Rb	68.35—115.91	78.36	0.100	62.88—83.66	74.73	0.06	50.51—113.95	84.50	0.14	112.00
Sr	208.11—328.92	274.68	0.080	143.99—489.31	277.98	0.22	91.77—256.96	166.33	0.24	350.00
Y	16.16—27.38	21.06	0.110	8.04—19.88	13.05	0.21	6.66—29.49	12.59	0.33	22.00
Zr	124.61—430.16	209.83	0.240	72.19—717.82	211.61	0.43	60.30—656.27	255.80	0.47	190.00
Nb	8.26—15.39	11.31	0.130	4.06—13.27	8.06	0.23	3.51—14.56	7.93	0.37	25.00
Ba	405.2—688.7	553.56	0.100	459.14—940.42	684.7	0.16	458.59—761.21	644.11	0.09	550.00
Ce	48.38—107.78	64.64	0.130	52.17—81.34	66.34	0.09	44.22—102.06	67.51	0.14	64.00
Nd	17.13—40.97	25.83	0.190	8.00—32.24	19.24	0.27	2.05—33.93	14.64	0.39	26.00
Pb	12.23—24.00	14.89	0.11	8.29—10.87	11.52	0.12	/	6.92	0.73	20.00

The chemical index of alteration (CIA) can be calculated by Nesbitt and Young (1982), and the McLennan correction method of CaO is used in this paper (McLennan, 1993) . Nesbitt et al (1980) had developed A–CN–K/A-CNK-FM ternary diagrams to predict the continental chemical weathering trend. The direction from UCC to PASS on the diagram represents the typical trend of continental chemical weathering (Nesbitt et al, 1980; Nesbitt and Young, 1982; Nesbitt and Markovics, 1997; Chen et al, 2001) . From the A-CN-K and A-CNK-FM ternary diagrams (Fig.7), it is found that the data of samples for each basin concentrated in a group (Fig.7a), indicating that the sediments in different basins came from different matter sources, while sediments in the same basin came from similar matter sources. The weathering trendline of three basin was mostly paralleled with the CN–A boundary, and concentrated along the UCC weathering trend line, indicating that the chemical weathering trend of sediments for each basin had a high degree of consistency. All data of Keriya River and most data Mu Bulag River were less than UCC, contrastingly, almost all data of Xi Xar Moron River basin were higher than UCC but much lower than PAAS, indicating that the three basins were unaffected by continental chemical weathering or chemical weathering were in its weak initial stage (Honda and Shimizu, 1998; Cullers and Podkovyrov, 2000; Cullers, 2002), namely in the weak stage of Na and Ca removal. CIA values were usually less than 50 and decreased from west to east, and the corresponding chemical weathering degree decreased.

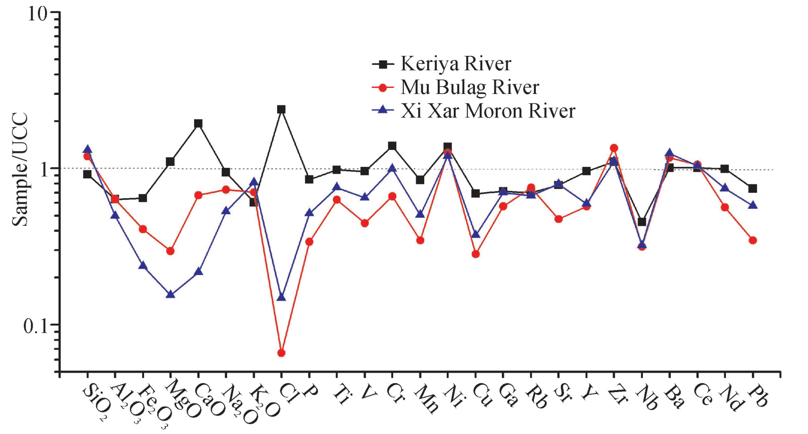

Fig.5　Chemical element UCC normalized value distribution plots in the three basins

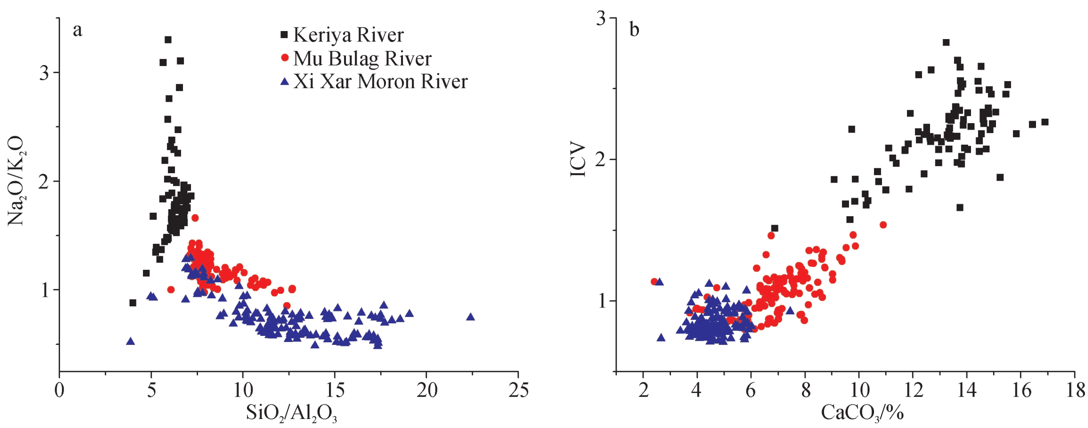

Fig.6　Scatter diagrams of SiO_2/Al_2O_3 vs Na_2O/K_2O (a), ICV vs $CaCO_3$(b) for the three basins

In the A-CNK-FM diagram, the content differences of Fe and Mg were used to determine the migration and enrichment of elements during the weathering and deposition process. As seen from Fig.7b, both the FM (Fe_2O_3 + MgO) content and the alkali metal (CNK) content decreased from west to east for three basins, while the Al content increased. The change trend of Fe and Mg contents in the Keriya River was basically unchanged (Fig.7b, Trend 1). However, the change trends in the Mu Bulag River and Xi Xar Moron River were obvious (Fig.7b, Trend 2). Due to their poor physical and chemical stability, the minerals enriched with Fe and Mg (biotite, amphibole) were easy for development. Thus, they underwent crushing and weathering from mechanical actions (abrasion, sorting) during deposition and transportation processes, indicating that mechanical weathering was the main cause of the Fe and Mg's removal from sediments in the three basins. In the western arid Keriya River, chemical weathering was weak, while in the central and eastern basins, which experience more rainfall, the chemical weathering rate was much higher than the wind transportation erosion rate, which caused losses of Na, Ca, Mg, and other elements from the surface sediments.

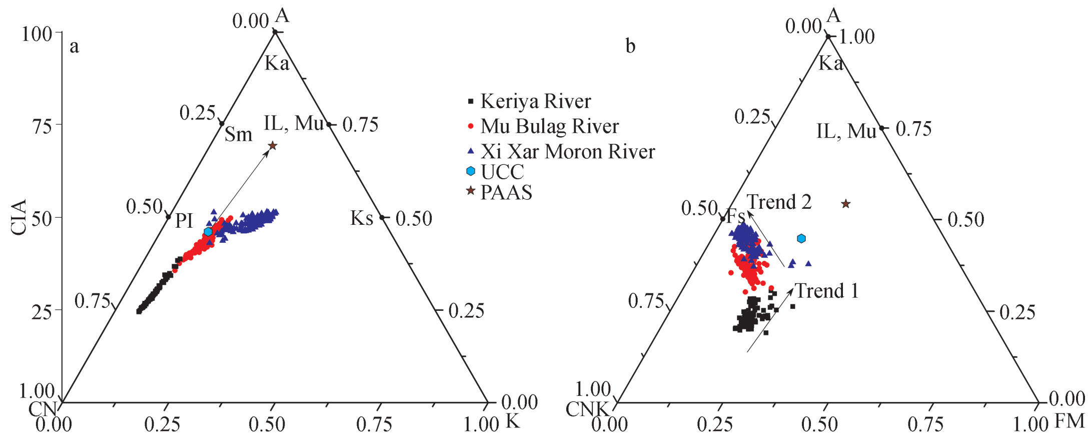

Fig.7 A-CN-K and A-CNK-FM ternary diagrams in the three basins
A: A1$_2$O$_3$, C: CaO, N: Na$_2$O, K: K$_2$O, F: Fe$_2$O$_3$, M: MgO, CaO: Molar content of silicate minerals, PI: Plagioclase, Ks: K-feldspar, Sm: Montmorillonite, IL: Illite, Mu: Muscovite, Ka: Laolinite, Fs: Feldspar.

4 Discussions

The drylands of China are caused by their remoteness from oceanic moisture and the blockage of moisture pathways by high mountains and plateaus. The degree of aridity changes gradually on a large-scale, resulting in both arid and semi-arid climate zones at the same latitudes. The factors controlling the composition of surface sediments included mainly the original rock, topography (tectonism and geology), climate and weathering processes (Babechuk et al, 2014). The key factors controlling the grain size characteristics or chemical weathering should be independent and occur at different spatial scales. The three basins studied in this paper included western, middle, and eastern regions of North China and were all large-scale watersheds. The climate primarily controlled the characteristic differences in surface sediments. These differences reflected the change rule of the physical and chemical characteristics of surface sediments from west to east and were relatively consistent within a given basin. For Keriya River in the west, the extremely arid environment drove the lack of surface biochemical processes, while the existence of obvious mechanical transformation by wind resulted in a high degree of sorting and mixing, fine grain size, well sorting, and narrow kurtosis. Its sediments experienced weak and consistent chemical weathering characteristics attributable to the elementary stages of chemical weathering. For Mu Bulag River in the middle and Xi Xar Moron River in the east, despite their different source regions and parent rocks, there were closer hydrothermal conditions and a similarity in physical weathering processes, resulting in coarse grain size, poor sorting, and wide kurtosis in sediments affected by surface water or groundwater. Their chemical characteristics were indicative of significant hydrogenic and chemical weathering processes. Therefore, the differences of sediment characteristics in the three basins can reflect wind or water dynamical sorting differences to some extent.

However, because the sediments were collected near the rivers, they experienced repeated cycles of erosion, transport, deposition by wind and water. On the one hand, these processes resulted in certain similarities in the grain size characteristics, reflecting the mixed distribution and difficult differentiation from grain size paraments. On the other hand, there were certain factors that controlled the grain size characteristics of the sediments, including weathering and the presence of other elements with more complex relationships (Honda and Shimizu, 1998; Daniel et al, 2004; Yang et al, 2004, 2013). Many studies have investigated the relationship between sediment grain size and geochemical processes (Roser and Korsh, 1986; Garzanti and Vezzoli, 2007; Yang et al, 2012). In this paper, we found that the chemical weathering degree was positively correlated with the average grain size, which correlation was more significant from west to east for the three basins, indicating that the grain size could control and influence the chemical weathering process to a certain extent. In addition, chemical weathering could also promote the grain adhesion or crushing, and the granularity effect was more obvious in the regions with higher chemical weathering degrees (Nesbitt and Young, 1982; Xiong et al, 2008; Yang et al, 2012). Therefore, the ability to effectively distinguish sediment transformation processes from physical and chemical weathering was key to determining the contribution rates of wind and water in the sediment migration process and to developing integrated discrimination indices of wind and water two-phase sediment. Starting with sedimentology, geology, geochemistry and others, related studies could be conducted using statistical analyses on small-scale areas with similar geographical conditions. Future research should focus on the following: analyzing the hydrological conditions, local topographical factors, relationships with river flow direction, wind direction, and the distance from the river in different river sections and different geomorphologic units in a basin; investigating the transformation of parent materials under the action of wind and water; defining the degree of change; determining how much information is inherited from the parent material; establishing effective identification indices; and determining the impact of the degree of transformation of the parent material on the recorded changes in hydrology, climate, geology, and other factors in a basin.

In addition, the results suggest that sand sources mainly relating to fluvial and alluvial processes are more important than other factors in explaining their occurrence in these arid environments. Continuous inflows of fresh sediments probably account for the dune materials being relatively unweathered, as shown by sedimentological and geochemical indicators. On a watershed large-scale, wind strength seems to have little influence on the occurrence of sediment on the different watershed of deserts. In reflecting on the various studies of the sand sources of the different deserts or sand lands in northern China, one has to keep in mind that geochemical data need to be interpreted within geomorphological contexts. Geomorphological settings and modern wind patterns as well as some geochemical indicators jointly support the opinion that the sands of the deserts are from local regions. It is unlikely that any of the sand seas were caused by incursions from another sand sea by aeolian processes.

5 Conclusions

In this paper, the grain size, mineral composition, and geochemical characteristics of surface sediments from the Keriya River, Mu Bulag River, and Xi Xar Moron River were analyzed, and sediment characteristics under wind and water interaction were discussed. The main conclusions were:

(1) The sediments in the three basins contained small amounts of clay and coarse sand. In the Keriya River, the sediment was primarily silt and very fine sand, and the sediments from the Mu Bulag River and Xi Xar Moron River basins were primarily fine sand and medium sand. From west to east for three basins, the average grain size coarsened, the sorting worsened, the skewness increased, the kurtosis widened, and the distribution balance reduced.

(2) The minerals in the three basins were mainly consisted of the light minerals of quartz and feldspar, with less heavy minerals. The heavy minerals were mainly derived from biotite and hornblende, with less epidote. From west to east for the three basins, the mineral maturity index (feldspar/quartz) decreased and the sediments transformation period decreased.

(3) With respect to the sediment chemical composition in the three basins, the content order of common oxidizes was Keriya River > Mu Bulag River > Xi Xar Moron River. Compared with UCC, there were depletions of common oxidizes with the exception of

SiO_2, MgO, and CaO (in Keriya River), and there were also depletions trace elements with the exception of Co and As. The variation coefficient of the common and trace elements were mostly moderate, and sorted as Xi Xar Moron River > Mu Bulag River > Keriya River.

(4) The common chemical indices and the A-CN-K ternary diagram indicated that the sediments in the three basins experienced low-level chemical weathering, with a certain equalization of chemical characteristics within each basin. ICV and $CaCO_3$ content can be also used as indices to divide boundaries of chemical weathering between the three basins, with increase of weathering degree from west to east. And the A-CNK-FM ternary diagram indicated that Fe and Mg elements in the three basins had a differentiation characteristic and revealed the relationship between chemical and mechanical weathering in arid and semi-arid areas.

(5) On the different watershed of deserts, sorting differences of the surface sediments caused by climate-induced aeolian and fluvial interactions were a key factor in forming zonal distribution of physicochemical characteristics for the surface sediments from the three basins. The low degree of chemical weathering is caused principally by extreme aridity, rapid rejuvenation of detrital sediments associated with strong aeolian processes, and an intensive input of fluvial deposits, as well as a lack of vegetation.

References

Babechuk M G, Widdowson M, Kamber B S. 2014. Quantifying chemical weathering intensity and trace element release from two contrasting basalt profiles, Deccan Traps, India [J]. *Chemical Geology*, 363: 56−75.

Bagnold R A, Barndorff-Nielsen O E. 1980. The pattern of natural size distributions [J]. *Sedimentology*, 27: 199−207.

Belnap J, Munson S M, Field J P. 2011. Aeolian and fluvial processes in dryland regions: the need for integrated studies [J]. *Ecohydrology*, 4: 615−622.

Biscaye P E. 1965. Mineralogy and sedimentation of recent deep-sea clay in the Atlantic Ocean and adjacent seas and oceans [J]. *Geological Society of America Bulletin*, 76: 803−832.

Bullard J E, Livingstone L. 2002. Interactions between aeolian and fluvial systems in dryland environments [J]. *Area*, 34: 8−16.

Bullard J E, McTainsh G H. 2003. Aeolian-fluvial interactions in dryland environments: examples, concepts, and Australia case study [J]. *Progress in Physical Geography*, 27: 471−501.

Chen J, An Z S, Lin L W, et al. 2001. Variations in chemical compositions of the eolian dust in Chinese Loess Plateau over the past 2.5 Ma and chemical weathering in the Asian inland [J]. *Science in China (Series D)* , 44: 403−413.

Churchman G J. 2000. The alteration and formation of soil minerals by weathering [M]//Sumner M E. Handbook of Soil Science. Baco Raton: CRC Press: F3−F76. .

Cox R. 1995. The influence of sediment recycling and basement composition on evolution of mudrock chemistry in the southwestern United States [J]. *Geochimica et Cosmochimica Acta*, 59: 2919−2940.

Condie K C, Dengate J, Cullers R J. 1995. Behavior of rare earth elements in a paleoweathering profile on granodiorite in the Front Range, Colorado, USA [J]. *Geochimica et Cosmochimica Acta*, 59: 279−294.

Cullers R L, Podkovyrov V M. 2000. Geochemistry of the Mesoproterozoic Lakhanda shales in southeastern Yakutia, Russia: implications for mineralogical and provenance control, and recycling [J]. *Precambrian Research*, 104: 77−93.

Cullers R L. 2002. The source and origin of terrigenous sedimentary rocks in the Mesoproterozoic Ui group, southeastern Russia [J]. *Precambrian Research*, 117: 157−183.

Daniel R M. 2004. Mineralogical maturity in dunefields of North America, Africa and Australia [J]. *Geomorphology*, 59: 247−269.

Dobrovoljski B B. 1987. Trace Element Geography [M]. Zhu Y M, translated. Beijing: Science Press: 144−152.

Draut A E. 2012. Effects of river regulation on aeolian landscapes, Colorado River, southwestern USA [J]. *Journal of Geophysical Research*, 117, F02022, doi: 10.1029/2011JF002329.

Field J P, Breshears D D, Whicker J J. 2009. Toward a more holistic perspective of soil erosion: why aeolian research needs to explicitly consider fluvial processes and interactions [J]. *Aeolian Research*, 1: 9−17.

Folk L. 1980. Petrology of Sedimentary Rocks [M]. Texas: Hemphill, Publishing Company: 182.

Folk R L, Ward W C. 1957. Brazos river bar: a study in the signification of grain size parameters [J]. *Journal of Sedimentary Petrology*, 27: 3−27.

Garzanti E, Vezzoli G. 2007. Quantifying sand provenancc and erosion (Marsyandi River, Nepal Himalaya) [J]. *Earth and Planetary Science Letters*, 258: 500−515.

Gile L H, Peterson F F, Grossman R B. 1996. Morphological and genetic sequences of carbonate accumulation in desert soils [J]. *Soil Science*, 101: 347−360.

Honda M, Shimizu H. 1998. Mineralogical and sedimentological studies on the Taklimakan Desert sands [J]. *Sedimentology*, 45: 1125−1143.

Lancaster N. 1989. The Namib Sand Sea: dune forms, processes, and sediments [J]. *Geographical Journal*, (1): 1−190.

Lancaster N. 1995. Geomorphology of desert dunes [M]. London: Routledge: 228−290.

Li E J. 2011. The contrast studies of desert sedimentary characteristic on regional scale between Badain Jaran Desert and Tenger Desert [D]. Xi'an: Shaanxi Normal University: 8−9.

Li C Z, Yang X P. 2004. Comparison research on sand deposit climate proxies in North China [J]. *Quaternary Research*, 24: 469−473.

McLennan S M. 1993. Weathering and global denudation [J]. *Journal of Geology*, 101: 295−303.

Muhs D R. 2004. Mineralogical maturity in dune fields of North America, Africa and Australia [J]. *Geomorphology*, 59: 247−269.

Nesbitt H W, Markovics G, Price R C. 1980. Chemical processes affecting alkalis and alkaline earths during continental weathering [J]. *Geochimica et Cosmochimica Acta*, 44: 1659−1666.

Nesbitt H W, Young G M. 1982. Early Proterozoic climates and plate motions inferred from major element chemistry of lutites [J]. *Nature*, 299: 715−717.

Nesbitt H, Markovics G. 1997. Weathering of granodioritic Ernst, long-term storage of elements in weathering profiles, and petrogenesis of siliciclastic sediments [J]. *Geochemical et Cosmochimica Acta*, 61: 1653−1670.

Nesbitt H, Young G. 1996. Petrogenesis of sediments in the absence of chemical weathering: effects of abrasion and sorting on bulk composition and mineralogy [J]. *Sedimentlogy*, 43: 341−358.

Ravi S, Breshears D D, Huxman T E, et al. 2010. Land degradation in drylands: interactions among hydrologic-aeolian erosion and vegetation dynamics [J]. *Geomorphology*, 116: 236−245.

Robinson R S, Johnsson M J. 1997. Chemical and physical weathering of fluvial sands in an arctic environment; sands of the Sagavanirktok River, North Slope, Alaska [J]. *Journal of Sedimentary Research*, 67: 560−570.

Roser B P, Korsch R J. 1986. Determination of tectonic setting of sandstone-mudstone suites using SiO_2 content and K_2O/Na_2O ratio [J]. *Journal of Geology*, 94: 635−650.

Thomas D S G. 1988. Analysis of linear dune sediment-form relationships in the Kalahari Dune Desert [J]. *Earth Surface Processes and Landforms*, 13: 545−553.

Tooth S. 2008. Arid geomorphology: recent progress from an earth system science perspective [J]. *Progress in Physical Geography*, 32: 81−101.

Tooth S, Nanson G C. 2011. Distinctiveness and diversity of arid zone river systems [M]// Thomas D S G. Arid zone geomorphology: process, form and change in drylands. 3rd ed. New York: John Wiley & Sons: 269−300.

Winspear N R, Pye K. 1995. Sand supply to the Algodones dunefield, south-eastern California, USA [J]. *Sedimentology*, 42: 875−891.

Xu Z W, Lu H Y, Zhao C F, et al. 2011. Composition, origin and weathering process of surface sediment in Kumtagh Desert, Northwest China [J]. *Journal of Geographical Sciences*, 21: 1062−1076.

Xiong S F, Zhu Y J, Zhou R, et al. 2008. Chemical weathering intensity and its grain-size dependence for the loess-red clay deposit of the Baishui section, Chinese Loess Plateau [J]. *Quaternary Sciences*, 28: 812−821.

Yang X P, Karl T R, Frank L, et al. 2004. The evolution of dry lands in northern China and in the Republic of Mongolia since the Last Glacial Maximum [J]. *Quaternary International*, 118/119: 69−85.

Yang X P, Wang X L, Liu Z T, et al. 2013. Initiation and variation of the dune fields in semi-arid northern China – with a special reference to the Hunshandake Sandy Land, Inner Mongolia [J]. *Quaternary Science Reviews*, 78: 369−380.

Yang X P, Zhu Z D, Jaekel D, et al. 2002. Late Quaternary palaeoenvironment change and landscape evolution along the Keriya River, Xinjiang, China: the relationship between high mountain glaciation and landscape evolution in foreland desert regions [J]. *Quaternary International*, 97/98: 155−166.

Yang X F, He D F, Wang Q C, et al. 2012. Provenance and tectonic setting of the Carboniferous sedimentary rocks of the East Junggar Basin, China: evidence from geochemistry and U-Pb zircon geochronology [J]. *Gondwana Research*, 22: 567−584.

Yang X P, Li H W, Conacher A. 2012. Large-scale controls on the development of sand seas in northern China [J]. *Quaternary International*, 250: 74−83.